

Surface and Interior Measurements of Grain Boundary Sliding During Creep

R. L. BELL

Engineering Laboratories, The University, Southampton, UK

C. GRAEME-BARBER

Central Electricity Research Laboratories, Leatherhead, UK

Measurements of grain boundary sliding have been made on polycrystalline specimens of Magnox AL80, a magnesium-0.78 wt% aluminium alloy, at successive strains during creep at 200°C under a stress of 2800 psi. Three independent methods were used to determine the strain due to sliding (ϵ_{gb}) at the surface and two to determine ϵ_{gb} in the interior of the specimens. The one direct method of measuring ϵ_{gb} in the interior used oxide markers introduced by extruding a composite billet. The values of ϵ_{gb} obtained from the offsets in these interior markers were found to agree with those given by the three sets of measurements made on the surface, but not with those from the indirect method for the interior which relies on the measurement of grain strain via grain shape changes.

1. Introduction

The estimation of the overall strain due to sliding at the individual grain boundaries in a polycrystal is a problem fraught with numerous difficulties which have been the subject of two recent reviews [1, 2]. In addition to the difficulties of sampling associated with the non-randomness of boundary angles met by a linear traverse [3], and the fact that annealing or creep can modify the average angle at which grain boundaries meet a surface [4-6], there is the possibility that the role of grain boundaries in the interior of a polycrystal might be quite different from that at the surface [7]. Although Rachinger himself invented an internal marker method for revealing displacements at internal boundaries in aluminium, all of his estimates of grain boundary sliding in the interior relied on an indirect method, involving the evaluation of grain strain from grain shape changes. The subsequent criticism [8] that boundary migration would tend to maintain equiaxed grains and hence lead to an underestimation of grain strain and an overestimation of grain boundary strain was challenged by Rachinger [9] who showed that grain elongation produced, either by a previous hot-rolling treatment, or by intermittent rapid strain at the creep temperature, was not removed during subsequent creep. However, these were not wholly satisfactory check experiments, for whereas the

spheroidisation of initially elongated grains would require boundary migration on a large scale, the maintenance of an equiaxed structure could be accomplished by localised migrations [10].

An independent assessment of the grain shape method was made by Langdon and Bell [11] who used a photographically printed grid for the determination of grain strain. These experiments showed that, at the surface of a specimen, the grain shape method tends to underestimate grain strain the more as the creep conditions favour grain boundary sliding and migration.

A possible criticism of the grid method for determining grain strain is that it ignores those parts of the grain which are immediately adjacent to the grain boundaries; in these regions the deformation behaviour may be different from that in the centre of a grain. The only relevant evidence on this point is that obtained by Gifkins [12] who showed that in lead bicrystals the slip in the vicinity of the boundary was "accommodating slip" which contributed nothing to the overall strain. If this were generally true, the grid method would overestimate the grain strain, but only in the proportion of the width of this zone (or of the distance between the grid line and the nearest boundary, whichever is the smaller) to the grain diameter. In Gifkins' bicrystal experiments this zone of accommodat-

ing slip was about 0.3 mm wide, but in a polycrystal it is likely to be only a few microns wide and the error in ϵ_{gb} , therefore, very small.

The validity of the grain shape method for the determination of the behaviour in the interior of a specimen has only been checked once by an independent method: Ishida *et al* [10] developed the internal marker technique for aluminium and found that the contribution of grain boundary sliding to the total strain was approximately the same in the interior as at the surface. This conclusion is not invalidated by the omission of a factor of 2 [13] in the formula they used to determine the grain boundary strain, because the same formula was used for both interior and surface estimates. However, since Ishida *et al* only investigated the one material under a very limited range of conditions, there was a clear need for further evidence on this important controversy.

In the present work a magnesium-0.78 wt % aluminium alloy, "Mgnox AL80", was subjected to slow creep at 200°C (0.5 T_m approx.) and the sliding contribution measured both at the surface and in the interior by a number of independent techniques.

2. Formulae for the Strain due to Boundary Sliding

Fig. 1 illustrates how u , the elongation in the direction of the stress axis, due to sliding on a single boundary may be described in terms of the components v , and w and the angles θ and ψ .

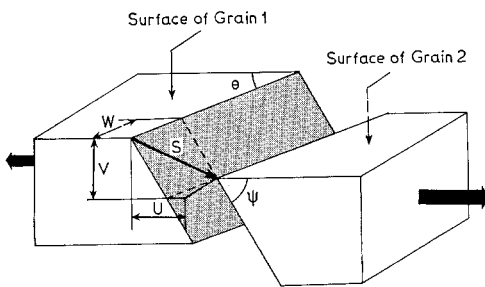


Figure 1 Schematic representation of grain boundary sliding.

To obtain the elongation, ϵ_{gb} , due to the sliding at all the boundaries in a polycrystal it is simplest, in principle, to sum the values of u measured at every boundary intersected by a line drawn parallel to the stress axis [3, 7]. This sum may be expressed:

$$\epsilon_{gb} = \frac{1}{l_0} \sum_0^l u \quad (1)$$

or

$$n_l \bar{u}_l \quad (1a)$$

where l is the length of the longitudinal traverse (whose original length was l_0) along which the values of u are summed, n_l is the number of grains per unit length along a longitudinal traverse in the unstrained sample, and \bar{u}_l is the average value of u obtained by summation along a longitudinal traverse. In practice it is difficult to use this method because the points of intersection of a longitudinal marker line with the grain boundaries become obscured due to boundary migration. Brunner and Grant [3] devised a means of overcoming this problem which involves the summing of u values along a transverse marker line of length t . In this case the measurement of the offsets u does not require the precise location of the points of intersection of the marker with the grain boundaries, but to take account of the different distribution function for the orientation of boundaries intersected by a transverse traverse, as opposed to a longitudinal traverse, Brunner and Grant derived the formula:

$$\epsilon_{gb} = \frac{1}{t} \sum_0^t u \tan \theta \quad (2)$$

or

$$n_t (\overline{u \tan \theta})_t$$

where the subscripts denote averages obtained along a transverse traverse. The derivation of this equation involved various assumptions which have been shown [14] to limit its use to the very special case where grains start, and remain equiaxed, i.e. where no grain strain occurs, so it is fortunate that the alternative empirical procedure suggested by Couling and Roberts [15] does not have these limitations. They used transverse marker lines to obtain average values of u at each of a series of values of θ , and then determined the distribution function $f_i(\theta)$ for the boundary angles intersected by a longitudinal traverse so as to calculate the mean value of u that would be encountered by a longitudinal traverse, i.e. \bar{u}_l for insertion into formula 1a.

Measurements of the components v and w

may be made at each grain boundary intersected by a longitudinal traverse and, in principle, these may be used in the appropriate form of formula 1 which is:

$$\epsilon_{gb} = \frac{1}{l_0} \sum_0^l \left(\frac{v}{\tan \psi} + \frac{w}{\tan \theta} \right) \quad (3)$$

Because of the difficulty of measuring the internal angle ψ this formula is not very useful in practice. However, in the interior of a polycrystal the difference between v and w is simply one of definition so that formula 3 becomes

$$\epsilon_{gb} = \frac{2}{l_0} \sum_0^l \frac{w}{\tan \theta} \quad (4)$$

or

$$2n_l \left(\frac{w}{\tan \theta} \right)_l$$

Another method for obtaining ϵ_{gb} relies on the assumption that

$$\epsilon_t = \epsilon_{gb} + \epsilon_g \quad (5)$$

where ϵ_t is the total strain and ϵ_g that due to deformation processes within the grains. This formula is subject to the provisos that engineering strains are only additive at small strains, and that there is no contribution other than sliding to the strain developed in the boundary regions. Under these conditions measurements of ϵ_t and of the grain strain – obtained say from observations of the change in shape of the grains [7, 16, 17] or by the use of a photographically printed grid [11, 18] – may sometimes be used to give ϵ_{gb} . Values of ϵ_{gb} obtained in this way have also been used [19] to obtain the empirical constant k for use in the formula:

$$\epsilon_{gb} = k n_r \bar{v}_r \quad (6)$$

where n_r is the number of grains per unit length before deformation, \bar{v} is the average value of v , and the subscript r denotes the procedure of averaging along a number of randomly directed lines.

3. Materials and Experimental Procedure

The alloy used in this investigation, Magnox AL80, was supplied by Magnesium Elektron Ltd together with the following analysis: 0.78 wt % aluminium, < 400 ppm impurities, remainder magnesium. It was obtained in the form of a 5.6 cm diameter bar which had been

extruded from a 30 cm diameter billet at 425°C. From this starting material a 1.25 cm diameter rod containing several sets of oxide markers was produced by a further extrusion process involving a composite billet consisting of a cylindrical can (5.6 cm o.d., 5.0 cm i.d.) filled with 3 mm thick 5 cm diameter discs all made from the 5.6 cm diameter Magnox bar. Details of this technique have been published previously [19]. The 20:1 extrusion ratio resulted in a sound rod in which the thin oxide from the surface of the discs had been broken up, thus allowing good welding, and distributed along the surface of greatly elongated paraboloids whose axes were parallel to the extrusion direction. Creep specimens were machined from this rod to the dimensions shown in fig. 2. The flat surfaces of

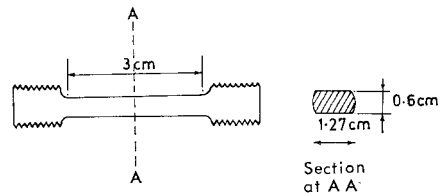


Figure 2 Dimensions of creep specimens.

the gauge length were intersected at approximately normal incidence by about twelve longitudinal planes containing markers. The individual 1 μm diameter oxide particles were in strings about 100 μm long, and after a final grain stabilisation treatment at 590°C for 2 h most of the strings appeared to have little or no influence on the orientation of the grain boundaries (see section 4.6 for more specific information on this point). A specimen without markers was prepared from 1.25 cm diameter rod which was obtained from an extrusion process identical to that used for producing the material with oxide markers, save that a solid billet was used instead of a composite one. The same stabilisation treatment was used and in both cases it resulted in a coarsening of the grain size from 30 μm in the extruded condition to 200 μm after stabilisation.

Oxidation during the stabilisation anneal was minimised by the use of a closely fitting sealed tube. Any surface oxide produced was removed by careful grinding, followed by an electropolish, and an etch in 4% Nital which also revealed the grain boundaries and the markers. Grain size measurements were made along traverses parallel

and perpendicular to the cylindrical axis of the specimen, as well as along randomly directed traverses. In each case forty different fields totalling more than 2000 intercepts were counted so that the grain dimensions were obtained to within 1 to 2% at the 95% confidence level. It was noted that although the grains were uniform in size they were elongated some 2 to 8% in the extrusion direction even after the stabilisation anneal. Before creep testing the etched surface was smoothed by a second electropolish and on one of the flat longitudinal faces an accurately spaced grid (79 lines per cm) was printed [18].

Creep tests were performed in constant load creep machines at a temperature of 200°C. In order to make measurements of grain strain and grain boundary sliding, the loading was interrupted at intervals and the specimen removed from the machine. On that face of the specimen having the superimposed photographic grid, measurements of the grain strain were obtained from the separation of pairs of grid lines not separated by a grain boundary. An accuracy of $\pm 10\%$, with 95% confidence limits, was obtained by taking 300 separate measurements on each occasion. For comparison with these estimates the grain strain of individual grains [17] was obtained from the change in their shape, and averages taken over 300 grains. However, this procedure only gave a reasonable standard error ($\leq 12\%$) when grain strains approached 4%. The v measurements were made using a two-beam interference microscope when the steps were $\leq 1 \mu\text{m}$, and a projection microscope fitted with a calibrated fine focusing knob when they were $\geq 1 \mu\text{m}$. On this surface having the photographic grid, u and w measurements could be made either from the offsets in grid lines or from those in oxide marker lines. In practice it was more convenient to use the former.

The flat surface of the gauge length opposite to that having the superimposed photographic grid was mechanically electro-polished to remove a depth of at least 3 grains every time a creep test was interrupted, and measurements of u and w made from discontinuities in the oxide marker lines to determine grain boundary sliding in the interior. The length to breadth ratio and hence the grain strains in 300 individual grains were averaged to give an independent value of the grain strain in the interior, but again this only gave a reasonable standard error when grain strains approached 4%.

Measurements of u , v , w were always made at

300 individual boundaries and these gave error bars on a mean of between 10 and 20% within 95% confidence limits. Values of ϵ_{gb} obtained via equation 4 should be within these limits. Those obtained via equation 6 will have, in addition, the uncertainty in the empirical constant k . At small strains where there was no cavitation this error was of order 10% making a total error in ϵ_{gb} of 20 to 30%. With estimates of ϵ_{gb} obtained via the Couling and Roberts procedure the error depends on the weighting given to the error in u at a particular θ by the distribution function $f_i(\theta)$, and on uncertainties in this function. It is estimated that the values of ϵ_{gb} obtained from the total of 300 u and θ measurements were within 30 to 40% at the 95% confidence level.

4. Experimental Results

4.1. Preliminary Experiments to Find Conditions Giving $\epsilon_{gb}/\epsilon_t \sim 50\%$

To enable a comparison between direct measurements of ϵ_{gb} and values obtained via grain strain (ϵ_g) measurements it was desirable that ϵ_{gb} and ϵ_g should be approximately equal so that the two could be determined with similar accuracy. To this end a series of preliminary tests was carried out to find conditions that gave $\epsilon_{gb} \approx \epsilon_g$. The results of Bell and Langdon [6] served as a useful guide but since the mechanical and thermal histories of the present specimens were somewhat different from theirs there were small but significant differences in the creep behaviour of specimens having the same final grain size. Thus the higher temperature of the grain stabilisation anneal in the present experiments, produced slightly softer grains which resulted in a higher creep rate, and smaller ratio ϵ_{gb}/ϵ_t than in nominally identical tests in the previous experiments. The conditions found to produce $\epsilon_{gb} \approx \epsilon_g$ were: applied stress 2800 psi, temperature 200°C.

4.2. Creep Curves

All the results described in this paper were obtained on three specimens which were creep tested under the conditions named above, namely 2800 psi 200°C. Two of the specimens, CB10 and CB11 contained oxide markers, and the histories of these two were identical, save that CB11 was heat treated for 2 h at 400°C after the final electropolish, which followed the grain stabilisation anneal at 590°C. The purpose of this 400°C treatment was to produce an "annealed" con-

figuration of grain boundaries at the surface [6], whilst avoiding the oxidation produced by a 590°C treatment. Apart from this change of surface configuration the structure of this "annealed" specimen CB11, would be expected to be identical to that of CB10 which was tested in the "cut" (or, to be precise, electropolished) condition. As a check the grain size of CB11 was measured after the final 400°C treatment and found to have been unchanged by it. The third specimen, CB9, was one without markers. It was tested in the "cut" condition.

Creep curves for these three specimens are reproduced in fig. 3. The two containing oxide

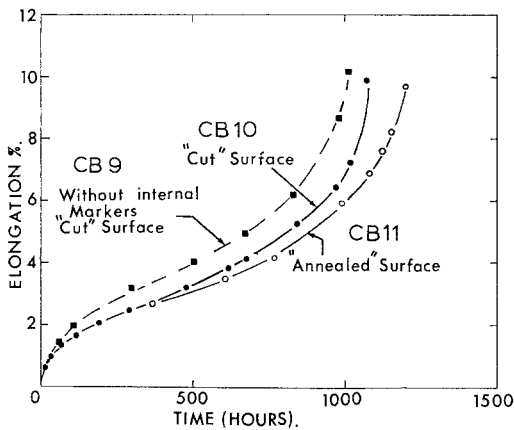


Figure 3 Creep curves for two specimens with internal markers (CB10 and CB11), and one without (CB9). Experimental errors on the strain measurements are indicated by the size of the points (namely $\pm 0.1\%$).

markers behaved in a closely similar fashion until well into secondary creep, but the one without oxide markers elongated a little more rapidly from the start. The oxide markers appear to have produced a small but noticeable stiffening effect on the overall creep characteristics. The relevance of this to the comparison of the sliding behaviour will be considered later.

4.3. ϵ_{gb} via Surface Measurements of u

The difficulty of summing u offsets along a longitudinal traverse (by making u measurements from the separation of the ends of a longitudinal line at each point where it crosses a boundary) in order to obtain ϵ_{gb} via the simple and soundly-derived formula 1 is best illustrated by an example: When specimen CB11 had been strained a total of 9.7%, 300 measurements of u obtained from the points of intersection of a longitudinal line with the grain boundaries gave $\bar{u}_t = 8.95 \pm 3.6 \mu\text{m}$ or an error of $\pm 40\%$ at the 95% confidence level. This very large error is attributed to the uncertainty in the position of the intersections caused by boundary migration. The difficulty is avoided by measuring u from the offsets in transverse markers. For example, the error on 300 measurements of u_t at $\epsilon_t = 9.7\%$ in specimen CB11 was only $\pm 16\%$.

Accordingly u measurements were made at successive boundary intersections along the transverse bars of the photographic grid of both cut and annealed specimens. θ -measurements were also made at each boundary intersection so that ϵ_{gb} could be calculated using the Brunner

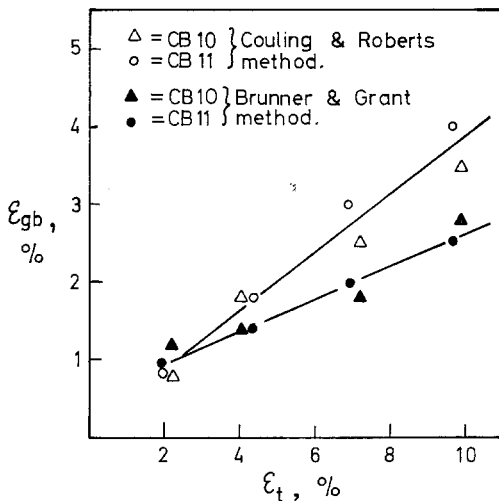
TABLE I Specimen CB10 ("cut" surface)

τ , h	ϵ_t , %	\bar{v}_r , μm	$(\epsilon_t - \epsilon_{grid})$, %	k expt.	ϵ_{gb} % using \bar{v}_r and $k = 1.1$	ϵ_{gb} , % (C and R)	ϵ_{gb} , % (B and G)	ϵ_{gb} , % (w_l surface)	ϵ_{gb} , % (w_l interior)
1	0.21	0.22			0.13				
8	0.65	0.66			0.40				
15	0.73	0.80			0.48				
31	1.00	1.1			0.68				
79	1.32	1.45			0.87				
123	1.74	1.9			1.1			1.0	1.0
194	2.16	2.1	1.2	1.1	1.2	0.8	1.2	1.15	1.4
291	2.47	2.5			1.5				
668	4.14	2.8	1.7	1.1	1.7	1.8	1.4	1.9	2.15
839	5.34								
976	6.44								
1026	7.23	4.9	3.5	1.3	3.5	2.5	1.8	3.15	2.6
					($k = 1.3$)				
1074	9.93	5.1	5.2	1.5	3.6	3.5	2.8	4.4	3.4
					($k = 1.3$)				

TABLE II Specimen CB11 ("annealed surface")

τ , h	ϵ_t , %	\bar{v}_r , μm	$(\epsilon_t - \epsilon_{grid})$, %	k expt.	ϵ_{gb} % using \bar{v}_r and $k = 1.1$	ϵ_{gb} , % (C and R)	ϵ_{gb} , % (B and G)	ϵ_{gb} , % (w_l surface)	ϵ_{gb} , % (w_l interior)
2	0.39	0.28			0.19				
12	0.75	0.50			0.36				
36	1.18	0.88			0.63				
183	1.95	1.74	1.3	1.4	1.25	0.8	0.9	0.9	1.0
368	2.66	2.09	1.4	1.2	1.4				
771	4.15	3.14	2.2	1.3	2.2	1.9	1.35	2.3	2.0
1081	6.94	4.18	3.5	1.5	3.0	3.0	1.95	3.6	3.3
1205	9.73	4.15	6.0	2.1	3.0	4.0	2.5	4.7	3.2

and Grant procedure (formula 2) or that devised by Couling and Roberts. The results obtained by the two procedures at a series of total strains are detailed in columns 7 and 8 of each of tables I and II, and summarised in fig. 4.

Figure 4 ϵ_{gb} obtained via u measurements on the surface.

In comparing the four sets of results shown in fig. 4 the first important feature to notice is that if the results obtained by either procedure are considered separately, the sliding obtained on the cut and annealed specimens is the same at each value of the total strain. Comparing results from the different methods, however, there is a consistent tendency, which increases in magnitude with increasing total strain, for the formula 2 to give the smaller estimate of sliding. This effect is not outside the estimated limits of error on the individual points, but the consistency of its sign led to a re-investigation of the derivation of this formula and the recognition that it is based on implicit assumptions that are valid only in an

extreme case [14]. The $\tan \theta$ arises as the ratio of the distribution functions for longitudinal and transverse traverses, which are sine θ and cosine θ , respectively, for equiaxed grains. Thus unless grains start with, and maintain, an equiaxed shape (i.e. there is no grain strain) the formula will not hold. Figs. 5a and b show that in the present case the distribution functions showed marked deviations from the simple sine and cosine relations as the total strain increased, but the nature of these deviations and the shape of the $\bar{u}(\theta)$ curve, fig. 5c, are so complex that it is not immediately obvious what the error in the calculation of ϵ_{gb} via formula 2 will be. One can simulate the Brunner and Grant procedure using the data in figs. 5b and c and confirm that in this particular case the result is an underestimation of ϵ_{gb} , but aside from the desirability of placing a limit on the likely error it seems pointless to investigate the matter further because any correction procedure would require an independent measure of $f_i(\theta)$ (or of the grain shape from which one might deduce $f_i(\theta)$) and given this one has all the necessary data for the more reliable Couling and Roberts computation.

4.4. ϵ_{gb} via v Measurements

Values of \bar{v}_r for use in formula 6 were obtained at selected total creep strains for each of the three specimens whose creep curves are shown in fig. 3. The results which are detailed in tables I to III show that at corresponding values of total creep strain the \bar{v}_r sliding component was always greater for the two specimens with cut surfaces (namely CB10 which contained oxide markers, and CB9 which did not) than for the specimen CB11 (also containing oxide markers) with an annealed surface. This effect, which has been noted previously [6] and ascribed to the marked change in the angle ψ that occurs during the

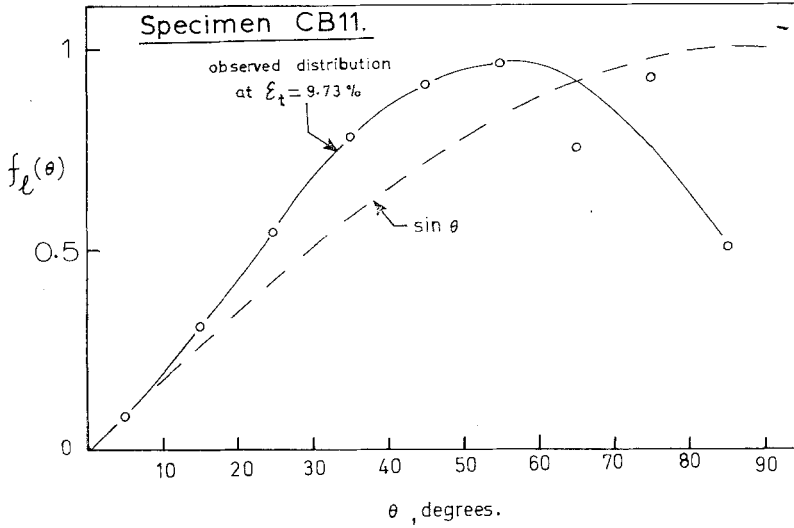
early stages of creep of a specimen with a cut surface, is thought to cause the constant k in formula 6 to change during the early stages of creep of a specimen with a cut surface [11].

Independent estimates of k were obtained empirically by measurement of the grain strain, ϵ_g , and formula 5. It became evident that at large total strains this formula needed to be modified to take account of the strain due to cavitation, ϵ_{cav} . The measurements of ϵ_g and

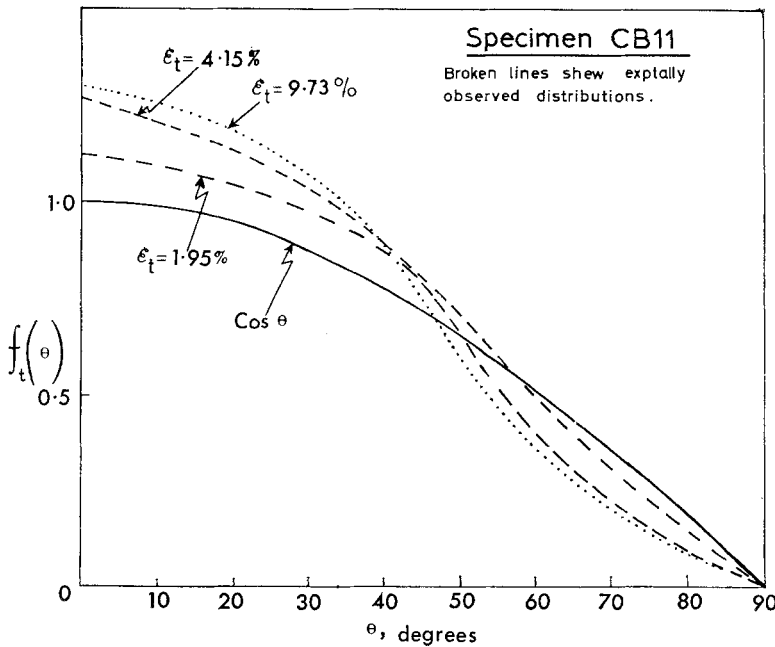
ϵ_{cav} are presented in the next two sections and the empirical values for k in section 4.4.3.

4.4.1. Grain Strain Measurements

Estimates of grain strain were obtained (a) from changes in the dimensions of the printed grid, and (b) from grain shape changes. Measurements of the latter were made both at the surface and in the interior of specimens, but even with the modified procedure suggested by Sellars [17] a



(5a)



(5b)

TABLE III Specimen CB9 (no markers, "cut" surface)

τ, h	$\epsilon_t, \%$	$\bar{v}_r, \mu m$	$(\epsilon_t - \epsilon_{grid}), \%$	k expt.	ϵ_{gb} , using \bar{v}_r and $k = 1.1$
1	0.35	0.27			
6	0.50	0.40			
30	0.75	0.68			
57	1.45	1.3			
105	1.81	1.75	0.59	1.04	1.1
298	3.21	2.5			
509	4.09	2.6			
831	6.21	3.7			
975	8.74	4.5			

TABLE IV Grain strain measurements

Specimen	$\epsilon_t, \%$	$\epsilon_g, \%$ from surface grid	$\epsilon_g, \%$ from grain shape at surface	$\epsilon_g, \%$ from grain shape in interior
CB10	2.16	0.96±0.07		
	4.14	2.4±0.2		
	7.23	3.7±0.4		
	9.93	4.7±0.6	3.9±0.5	3.2±0.4
CB11	2.76	1.25±0.08		
	4.15	2.0±0.2		
	6.94	3.4±0.4		
	9.73	3.7±0.4	3.1±0.4	2.6±0.4

reasonable accuracy was only obtained at the largest creep strains, where the grain strain was of order 3 to 4%. In table IV the results are summarised and it is seen that although for each specimen the two independent surface measurements of grains strain are just within the combined error bars, the values obtained from the grain shape measurements are in both cases lower than the corresponding values obtained from the printed grid, whilst those from interior grain shapes are quite significantly smaller than the surface grid values.

4.4.2. Strain due to Cavity Formation

If the processes of cavity nucleation and growth were wholly due to grain boundary sliding associated with a ledge or non-wetting particle the extension of the specimen accompanying cavitation would be accounted for by the sliding itself. However, there is strong evidence that vacancy condensation plays a major role in cavity growth [20]. Where this is the case an additional term, ϵ_{cav} , is required in formula 5 to take account of the elongation that is additional to that due to grain-, and grain-boundary deformation, and formula 5 becomes

$$\epsilon_t = \epsilon_g + \epsilon_{gb} + \epsilon_{cav} \tag{7}$$

In any particular case the relationship between ϵ_{cav} and the degree of cavitation will depend on the mode of formation of the cavities as well as on their shape and distribution. For present purposes an upper bound for ϵ_{cav} is required. This would be obtained in the extreme case, where all the cavities were on boundaries at 90° to the stress axis, and their growth wholly due to vacancy condensation. Then ϵ_{cav} would be given simply by $\Delta v/v$, the fractional volume change accompanying cavitation.

Estimates of the volume change due to cavitation were made on specimens CB10 and CB11 at their terminal creep strains (~ 10%) (a) by measuring the density change, and (b) by estimating the area of cavities on a longitudinal section. The reduction in density due to cavitation was obtained by measuring the densities of a section cut from the gauge length and one cut from a shoulder. The area-, and hence volume-fraction occupied by the cavities on a carefully ground, but not etched, longitudinal section was determined by the method of lineal analysis using a Quantimet. Results found using each of

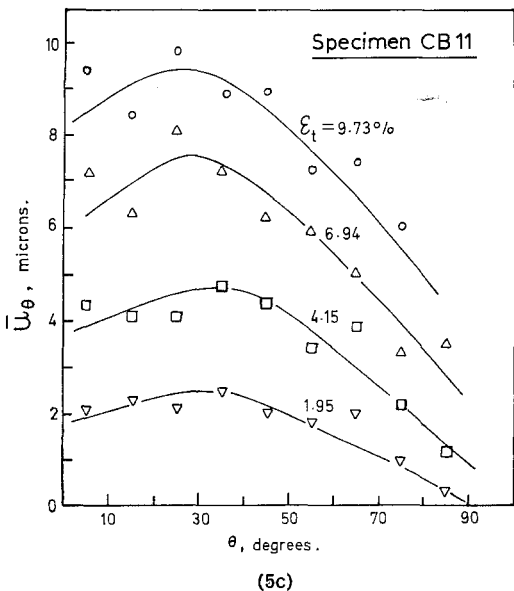


Figure 5 (a) The relative probability of finding boundaries of angle θ along a longitudinal grid line on the specimen surface. (b) The relative probability of finding boundaries of angle θ along a transverse grid line on the specimen surface. (c) The average value of u at a particular θ as a function of θ .

TABLE V Estimates of the degree of cavitation by density change measurements (column 3) and metallographic sectioning (column 4)

Specimen	ϵ_t , %	$\frac{-\Delta\rho}{\rho}$, %	$\frac{\Delta A}{A}$, %
CB10	9.9	1.0 ± 1.0	1.4 ± 1.4
CB11	9.7	1.2 ± 1.0	1.5 ± 1.1

these methods are shown in table V. For a particular specimen the agreement between the results obtained by the two different methods is well within the estimated errors, but in the next section the magnitude of these errors proves embarrassing.

4.4.3. Empirical Derivation of k

Estimates of the constant k in formula 6 were obtained by substituting the observed values of \bar{v}_r , ϵ_t and ϵ_g in formula 5 or \bar{v}_r , ϵ_t , ϵ_g and ϵ_{cav} in formula 7. Measured values of ϵ_{cav} were only available at the terminal creep strains because the experimental methods used for obtaining ϵ_{cav} involved sectioning the specimen; the values of ϵ_g used were, in all cases, those obtained via the photographic surface grid.

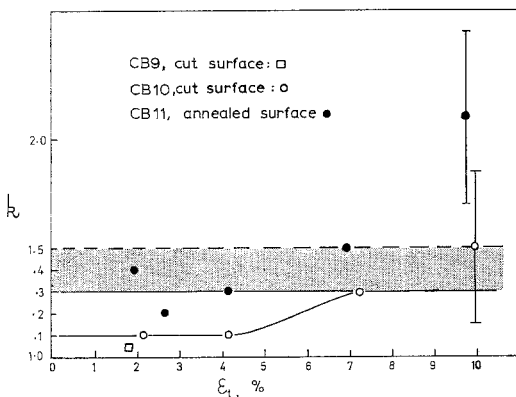


Figure 6 Empirical values of the constant k for use in formula 6, as a function of ϵ_t .

Fig. 6 shows the results obtained for k at each of several values of ϵ_t for the two specimens. At low total strains, where the estimation of ϵ_{cav} presents no problem because it is likely to be negligible, the previously noted difference between k for a cut, and for an annealed surface is clearly evident [11]. Since k is essentially a geometrical factor this difference is an expected consequence of the difference between the average values of ψ on cut and annealed surfaces. It follows that the value of k for the cut surface

should rise asymptotically toward that for the annealed surface, since during creep the grain boundary configuration changes in this way [6]. Unfortunately the present evidence on this point is not very precise because of uncertainties in the estimation of ϵ_{cav} .

In fig. 6 the points shown at the terminal creep strains were obtained by using the values of ϵ_{cav} given by the observed density changes, the limits shown corresponding to the estimated errors on these density change measurements. The limits allowed by the metallographic estimates of cavitation would be slightly greater.

An attempt to improve upon these errors was made by undertaking a second series of density measurements on fresh sections of the specimens and with a much more refined weighing technique. The results for the density difference between samples cut from gauge length and shoulder were 0.24 ± 0.09 and 0.96 ± 0.01 % for specimens CB10 and CB11, respectively. For CB11 the value corresponds quite closely with that obtained by the less exact weighing method, but for CB10 the much smaller density change observed would have the effect of shifting the point at $\epsilon_t = 9.73$ % in fig. 6 up towards the higher limit shown there. Since, however, the sample available from the gauge length was only a small one it is not certain that it was truly representative. In any case, the difficulties caused by the advent of cavitation are not limited to those associated with the measurement of a small relative change in density. They include also the uncertainties arising from the assumption that $\epsilon_{cav} = -\Delta\rho/\rho$ and that the surface and interior behaviour were the same. The latter difficulty could perhaps be overcome using the metallographic method, but the former difficulty would remain; the best chance of resolving this question of the terminal value of k would be obtained with a material that does not cavitate.

4.4.4. Values of ϵ_{gb} from v -measurements

The values in column 6 of tables I and II were obtained via formula 6 from measured values of \bar{v}_r and n_r using k values read off from the appropriate full-line curve in fig. 6. Where such a curve runs through an experimental point the ϵ_{gb} value computed from \bar{v}_r and n_r will, strictly, be independent of these values because the procedure then amounts to the following:

$$\epsilon_{gb} = \frac{\epsilon_t - (\epsilon_g + \epsilon_{cav})}{n_r \cdot \bar{v}_r} n_r \bar{v}_r.$$

4.5. ϵ_{gb} via w -measurements

Values of ϵ_{gb} were obtained via formula 4 by taking measurements both at the surface, and after removal of a layer of at least three grains thick, at each of a series of ϵ_t values from 2 up to 10%. These results are given in columns 9 and 10 of each of tables I and II. First it is important to note that the extent of sliding, as revealed by these w -measurements, was approximately the same in both cut and annealed specimens at each value of ϵ_t . Second, that ϵ_{gb} in the interior was, in every case, within experimental error equal to the corresponding value at the surface, although there was the suggestion of a tendency for the interior values to fall below those at the surface as ϵ_t increased. This is opposite to the effect which is apparent in the values of ϵ_{gb} (interior) found by substituting ϵ_g and ϵ_{cav} from grain shape and density measurements, respectively, in formula 7 – see table VI. However, the surface grid measurements of grain strain suggested that the grain shape technique underestimates ϵ_g and hence overestimates ϵ_{gb} . In table VI the comparison with ϵ_{gb} (surface) obtained via w gives independent confirmation of this point whilst the comparison with ϵ_{gb} (interior) obtained via w suggests that the underestimation is even greater in the case of interior measurements. Strictly it should be said only that the values obtained by the two techniques for obtaining ϵ_{gb} (interior) are different since we have no independent check of the marker method. However, the close agreement between the surface values of ϵ_{gb} obtained (a) via ϵ_{grid} and ϵ_{cav} and (b) via w indicates that the latter is reliable for surface estimates of ϵ_{gb} and, therefore, likely to be so for the interior too.

To check that the measurements made at three grain depths were typical of the bulk and not simply of a transition region intermediate between surface and interior, the two specimens CB10 and CB11 were finally sectioned longitudinally at a position close to the centre of their cross-section. The values of ϵ_{gb} obtained via w were 3.6 ± 0.7 and 3.2 ± 0.7 , respectively,

which are very close to those listed in table VI. Those obtained via grain shape were 7.1 ± 0.4 and 7.2 ± 0.3 , confirming the effect noted above, that the grain shape method overestimates ϵ_{gb} more severely in the interior.

4.6. Effect of the Oxide Markers

A comparison of the creep curves (fig. 3) showed that the oxide markers produced a small increase in the overall creep resistance. To check whether this was due to a pronounced effect on either the slip or sliding behaviour, measurements of both \bar{v}_r and grain strain were made on CB9 (no oxide markers) which had a printed grid on its cut surface. In section 4.4 the similarity of the sliding behaviour in CB9 and CB10 (which contained markers) was described. The surface grid measurements on CB9 showed that the grain strain behaviour was very similar too, e.g. at $\epsilon_t = 1.8\%$, $\epsilon_g = 0.85\%$ giving $\epsilon_{gb} = 0.95\%$ and $k = 1.04$. In other words the slight increase in overall creep resistance in the specimens with markers was not due to a particularly marked effect on grains or grain boundaries.

Since a very important objective in this work was to obtain reliable information on sliding behaviour in the interior of specimens, it was important to check whether the distribution functions for the angle of intersection made by boundaries with oxide stringers was typical of that along an arbitrarily chosen longitudinal traverse. In principle this need not matter since a formula such as 4 or 1 does not depend on the form of this distribution function provided the summation is made along a single longitudinal line; in practice a reasonably small statistical error on the mean can only be obtained by summing along a number of traverses, and in this case it is important that these traverses be typical. Figs. 7a and b show the results of measurements made to check this point. At $\epsilon_t = 1.74\%$ (fig. 7a) the three sets of points all lie close to the sine curve, showing that intersections with oxide markers (both at the surface and in the interior)

TABLE VI Surface and interior values of ϵ_{gb} at the terminal creep strain

Specimen	ϵ_{gb} at surface, %			ϵ_{gb} interior, %	
	via w	via grid*	via grain shape*	via w	via grain shape*
CB10	4.4 ± 0.7	4.2 ± 1.6	5.0 ± 1.5	3.4 ± 0.6	5.7 ± 1.4
CB11	4.7 ± 0.8	4.8 ± 1.4	5.4 ± 1.4	3.2 ± 0.6	5.9 ± 1.4

*These values were obtained via formula 7. The error in ϵ_{gb} due to uncertainty in ϵ_{cav} alone was $\pm 1\%$. If comparison between columns 3, 4 and 6 is made this error can be subtracted because the same ϵ_{cav} was used throughout for a given specimen.

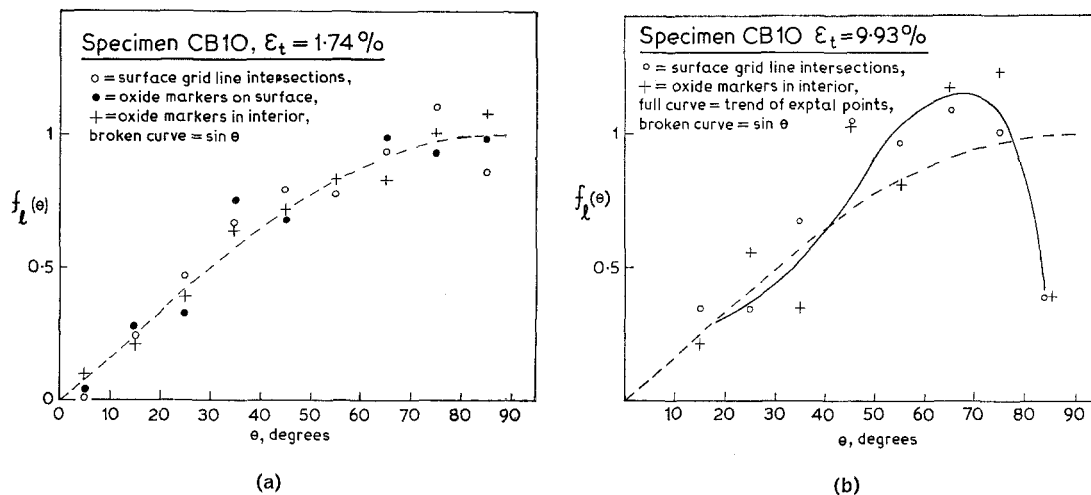


Figure 7 Comparison of the relative probability of finding boundaries of angle θ along a longitudinal traverse at surface and in interior. (a) at $\epsilon_t = 1.7\%$, (b) at $\epsilon_t = 9.9\%$.

follow the same distribution function as those with the arbitrarily located longitudinal lines of the photographic grid. At $\epsilon_t = 9.93\%$ the rumpling of the surface made it very difficult to check the distribution for the oxide marker intersections there, but the surface grid intersections and the internal oxide intersections both show the same sort of deviations from the sine law, although the experimental scatter is such that it is not possible to draw a very definite curve through either set of data. Despite this difficulty, it seems fair to conclude that at both extremes of ϵ_t the oxide marker intersections were typical of those along any arbitrarily chosen longitudinal traverse.

A further check on this point is afforded by data from specimen CB10 where at $\epsilon_t = 1.74\%$ the value of ϵ_{gb} (surface) was obtained by summing both along grid lines and along markers. The results: $\epsilon_{gb} = 0.95$ and 1.0% , respectively, show very close agreement.

5. Discussion

Fig. 8 summarises the results obtained for ϵ_{gb} as a function of total strain by all the different methods used, except the one relying on grain shape measurements for the determination of grain strain. The fact that at each value of ϵ_t the four measurements of ϵ_{gb} (three surface-, and one interior measurement) for each of two specimens agree within the estimated experimental errors implies firstly that the three surface methods are mutually self-consistent. Since the processing of the u -measurements by the Couling

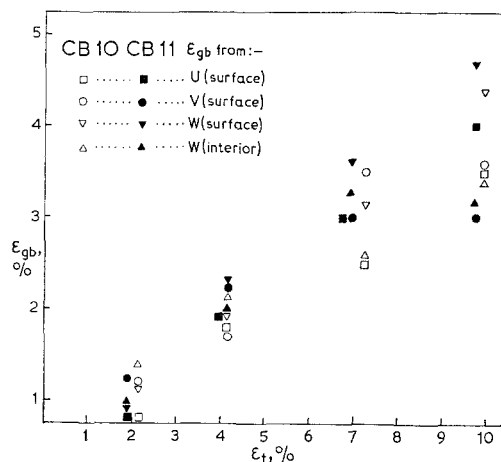


Figure 8 Comparison of results for ϵ_{gb} (surface) and ϵ_{gb} (interior).

and Roberts method makes no questionable assumptions and since the results are in agreement with those obtained by the wholly independent grain-strain method, it is considered that the three surface methods are not just self-consistent but reliable too. Hence the slightly doubtful assumption made in using equation 4 with surface measurements of w is validated.

A second point of note in fig. 8 is that there is no significant difference in the surface values of ϵ_{gb} as between specimens with cut and annealed surfaces. This is not surprising in the case of estimates based on the u or w components, but in the case of those based on v it arises only

because the smaller values of \bar{v}_r on the annealed specimen are compensated by the higher k .

The use of equation 4 with interior measurements of w involves a perfectly reasonable assumption and hence is expected to give reliable results. The conclusion follows that, under the conditions used in the present experiments, the strain due to grain boundary sliding in the interior was not significantly different from that at the surface. This confirms the conclusion of Ishida *et al* [10] who studied the situation in aluminium at about the same homologous temperature but under much faster creep rates than those used here. It is at variance with the early work of Rachinger [7], but not with that of Gittins [21], both of whom used the grain shape method for interior grain strain determination. However, this technique is considered unreliable for the reasons given earlier.

A possible way of obtaining independent confirmation of the w measurement of interior sliding would be to make u measurements using transverse oxide markers, but this would require two orthogonal sets of oxide markers or separate specimens. In any case, there is no good reason to doubt the validity of the present results, and the method based on formula 4 seems to be reliable and convenient – both for interior and surface sliding. Its one shortcoming is that it cannot be used when the offsets are less than about 2 μm . Here the use of v measurements is the only possibility, and the fact that the empirically derived values of the constant k in formula 6 are invariant with total strain between 2 and 4% gives confidence in using these two values (1.1 for “cut” surface, 1.3 for “annealed”) at smaller strains.

Since there is evidence [22] that the same values are also appropriate for aluminium, the v method could turn out to be a most convenient and generally useful one despite the complexity of its relationship with the other parameters [23]. The value of k at large strains needs further investigation because the problems associated with the estimation of ϵ_{cav} produced a rather large uncertainty here. In fig. 6 the spread of the experimental points suggests a value between 1.3 and 1.5. Using a terminal value of $k = 1.3$ for both cut and annealed specimens, values of ϵ_{gb} were obtained that agreed closely with those obtained by other methods, but it would be nice to have this result confirmed by experiments on a material that does not cavitate.

Acknowledgements

The experimental work described in this paper was carried out in the Metallurgy Department at Imperial College, London and the authors are grateful to Professor J. G. Ball for the provision of laboratory facilities there and to the Science Research Council for financial support in the way of a studentship for one of us (C. G-B.). Thanks are due to Mr C. Driscoll of the University of Southampton for the high precision density measurements referred to in section 4.4.3, and to Drs R. C. Gifkins and T. G. Langdon for helpful criticisms of the manuscript. The paper was completed during a sabbatical term spent by R.L.B. in the University of Cologne and thanks are extended to Professor H. Alexander for hospitality in the Abteilung für Metallphysik.

References

1. R. N. STEVENS, *TMS-AIME* **236** (1966) 1762.
2. R. L. BELL, C. GRAEME-BARBER, and T. G. LANGDON, *ibid* **239** (1967) 1821.
3. H. BRUNNER and N. J. GRANT, *ibid* **215** (1969) 48.
4. C. S. SMITH, *ibid* **175** (1948) 15.
5. A. GITTINS and R. C. GIFKINS, *Metals Sci. J.* **1** (1967) 15.
6. R. L. BELL and T. G. LANGDON, *J. Mater. Sci.* **2** (1967) 313.
7. W. A. RACHINGER, *J. Inst. Metals* **81** (1952-53) 33.
8. D. MCLEAN, “Grain Boundaries in Metals”, O.U.P. (1957).
9. W. A. RACHINGER, *Acta Metallurgica* **7** (1959) 374.
10. Y. ISHIDA, A. W. MULLENDORE, and N. J. GRANT, *TMS-AIME* **233** (1965) 204.
11. T. G. LANGDON and R. L. BELL, *ibid* **242** (1968) 2479.
12. R. C. GIFKINS, *J. Australian Inst. Met.* **8** (1963) 148.
13. R. L. BELL, C. GRAEME-BARBER, and T. G. LANGDON, *TMS-AIME* **233** (1965) 1648.
14. *Idem*, to be published.
15. S. L. COULING and C. S. ROBERTS, *TMS-AIME* **209** (1957) 1253.
16. J. H. HENSLER and R. C. GIFKINS, *J. Inst. Metals* **92** (1963-64) 340.
17. C. M. SELLARS, *ibid* **93** (1964-65) 365.
18. R. L. BELL and T. G. LANGDON, *J. Sci. Instr.* **42** (1965) 896.
19. C. GRAEME-BARBER and R. L. BELL, *J. Inst. Metals* **93** (1964-65) 551.
20. G. W. GREENWOOD, Proc. Int. Confce. on “Interfaces” (Ed. R. C. Gifkins, Butterworths 1969).
21. A. GITTINS, Ph.D. Thesis, Univ. Melbourne 1964.
22. T. G. LANGDON, private communication.
23. R. C. GIFKINS, A. GITTINS, R. L. BELL, and T. G. LANGDON, *J. Mater. Sci.* **3** (1968) 306.

Received 11 July and accepted 10 September 1970